Anal Bioanal Chem (2015) 407:8353–8362
DOI 10.1007/s00216-015-9020-8

RESEARCH PAPER

Clinical validation of surface-enhanced Raman scattering-based immunoassays in the early diagnosis of rheumatoid arthritis

Hyangah Chon[1] · Rui Wang[1] · Sangyeop Lee[1] · So-Young Bang[2] · Hye-Soon Lee[2] · Sang-Cheol Bae[2] · Sung Hyun Hong[3] · Young Ho Yoon[3] · Dong Woo Lim[1] · Andrew J. deMello[4] · Jaebum Choo[1]

Received: 30 July 2015 / Accepted: 31 August 2015 / Published online: 11 September 2015

Abstract We assessed the clinical feasibility of conducting immunoassays based on surface-enhanced Raman scattering (SERS) in the early diagnosis of rheumatoid arthritis (RA). An autoantibody against citrullinated peptide (anti-CCP) was used as a biomarker, magnetic beads conjugated with CCP were used as substrates, and the SERS nanotags were comprised of anti-human IgG-conjugated hollow gold nanospheres (HGNs). We were able to determine the anti-CCP serum levels successfully by observing the distinctive Raman intensities corresponding to the SERS nanotags. At high concentrations of anti-CCP (>25 U/mL), the results obtained from the SERS assay confirmed those obtained via an ELISA-based assay. Nevertheless, quantitation via our SERS-based assay is significantly more accurate at low concentrations (<25 U/mL). In this study, we compared the results of an anti-CCP assay of 74 clinical blood samples obtained from the SERS-based assay to that of a commercial ELISA kit. The results of the anti-CCP-positive group (n=31, >25 U/mL) revealed a good correlation between the ELISA and SERS-based assays. However, in the anti-CCP-negative group (n=43, <25 U/mL), the SERS-based assay was shown to be more reproducible. Accordingly, we suggest that SERS-based assays are novel and potentially useful tools in the early diagnosis of RA.

Keywords Surface-enhanced Raman scattering · Anti-CCP · Rheumatoid arthritis · Immunoassay · Early diagnosis

Published in the topical collection *Raman4Clinics* with guest editors Jürgen Popp and Christoph Krafft.

Electronic supplementary material The online version of this article (doi:10.1007/s00216-015-9020-8) contains supplementary material, which is available to authorized users.

✉ Jaebum Choo
jbchoo@hanyang.ac.kr

[1] Department of Bionano Technology, Hanyang University, Ansan 426-791, South Korea

[2] Department of Rheumatology, Hanyang University Hospital for Rheumatic Diseases, Seoul 133-792, South Korea

[3] EOne Laboratories, Songdo 406-840, South Korea

[4] Department of Chemistry and Applied Biosciences, Institute of Chemical and Bioengineering, ETH Zürich, Vladimir Prelog Weg 1, 8093 Zürich, Switzerland

Introduction

Surface-enhanced Raman scattering (SERS) is an emerging technique that allows sensitive, selective, and rapid biomarker detection [1–3]. For this reason, there is increasing interest in using SERS-based techniques in clinical diagnostics. A variety of biomarkers have already been quantitatively probed using a SERS-based immunoassay [4–8]. One of the most popular detection techniques using a SERS-based immunoassay incorporates a sandwich immunocomplex platform. Many different types of biomarkers, including immunoglobulin (IgG) antigens [2, 9, 10], feline calicivirus (FCV) [5], prostate-specific antigen (PSA) [11], protein A [12], hepatitis B virus [13], and mucin protein (MUC4) [14] have been studied using this SERS-based assay platform. Recently, a rapid SERS-based assay technique using magnetic beads has been developed [15–18]. This method uses magnetic beads as antibody supporting materials, and the sandwich immunocomplexes are immobilized on the wall of a microtube using a magnetic bar. This technique overcomes the slow immunoreaction problems caused by the diffusion-limited kinetics on a solid substrate, as the reaction occurs in a solution. As a result, the assay time is reduced to less than 1 h if properly designed metal nanotags are prepared. Furthermore, it is possible to achieve more reproducible results, because the

SERS signals are measured for the average nanoparticle ensembles in solution. However, the low concentrations of biomarkers in serums are the limiting factors to a diagnostic technique, so for SERS to be a practically useful method in the early detection of disease, it must be reproducible [19, 20].

Optimal conditions are needed to avoid aggregation and to enhance signals when metal nanoparticles are used in quantitative analysis. Aggregation leads to reduction in both SERS signals and reproducibility, and is difficult to control [21, 22]. To address the challenge posed by aggregation, hollow gold nanospheres (HGNs) were used as SERS nanotags [23–25]. HGNs are known to augment the SERS signal; the pinholes in the hollow structure of the particles can localize surface electromagnetic fields. The ability to enhance signals at a single particle level makes the HGN a very sensitive sensing probe in quantitative serum immunoassays.

A range of serum-based biomarkers have been tested for diagnostic purposes [26–28]. In fact, we have recently proposed the use of SERS-based immunoassays for the early diagnosis of rheumatoid arthritis (RA). In this work, an autoantibody against citrullinated peptide (anti-CCP) was used as a biomarker [29]. Various serum biomarkers were studied with regard to diagnosing RA. Anti-CCP autoantibodies are currently considered to be the best biomarkers in the early diagnosis of RA [30–33]. Specifically, we demonstrated that the SERS-based immunosensor is more sensitive at detecting human anti-CCP than is the commercially available enzyme-linked immunosorbent assays (ELISA). To assess the potential utility of SERS-based immunoassays as novel clinical tools in RA diagnosis, we used magnetic beads and HGN SERS nanotags for 74 clinical samples. Using a commercially available ELISA kit, the clinical samples were divided into anti-CCP-positive (n=31) and anti-CCP-negative (n=43) groups according to their assay results. Next, the SERS-based assay results were compared to those of the ELISA kit. Statistical analyses were used to evaluate the correlation between the ELISA and SERS-based assay results in both the anti-CCP-positive and anti-CCP-negative groups. There have been several reports about the application of a SERS-based assay for cancer and cardiac biomarkers [11, 23–25]. To the best of our knowledge, however, this is the first report about a SERS-based immunoassay for the anti-CCP detection in clinical samples. We anticipate that this new diagnostic technique satisfies the current need for the early diagnosis of RA.

Materials and methods

Reagents and materials

The following reagents were purchased from Sigma-Aldrich (St. Louis, MO, USA): gold(III) chloride trihydrate ($HAuCl_4 \cdot 3H_2O$), cobalt(II) chloride ($CoCl_2$), sodium borohydride ($NaBH_4$), trisodium citrate dehydrate ($HOC(COONa)(CH_2COONa)_2 \cdot 2H_2O$), poly(ethylene glycol) 2-mercaptoethyl ether acetic acid (HS-PEG-COOH, MW ~3500), *N*-(3-dimethylaminopropyl)-*N*′-ethyl carbodiimide hydrochloride (EDC), *N*-hydroxysuccinimide (NHS), and anti-human immunoglobulin G (IgG). The following additional reagents were purchased from Invitrogen (Eugene, OR, USA): malachite green isothiocyanate (MGITC), phosphate-buffered saline (PBS, 10×, pH 7.4), and streptavidin-coupled magnetic beads (Dynabeads® MyOne™ Streptavidin C1). Biotinylated second-generation cyclic citrullinated peptide (CCP) was purchased from Roche Diagnostics (Mannheim, Germany). The ELISA kit (Immunoscan, CCPlus) for the anti-CCP assay was purchased from Euro Diagnostica (Malmo, Sweden).

HGN preparation and antibody conjugation

The HGNs had already been prepared by standard methods [34, 35]. Cobalt nanoparticles that were synthesized using $CoCl_2$ reduced with $NaBH_4$ under N_2 gas were used as the templates. Gold nanoparticles were synthesized by nucleation and expansion over the cobalt base, and the hollow interior was obtained by the dissolution of the cobalt templates. $HAuCl_4$ was used at varying concentrations to control the thickness of the HGN walls. The average diameter and thickness of the walls were determined using transmission electron microscopy (TEM) measurements and were found to be 45± 12 and 15±5 nm, respectively.

The SERS nanotags were prepared according to the previously described procedure. In the first step, 1 μL of 5×10^{-5} M MGITC (Raman reporter) was introduced into the solution of 1.0 mL, 0.7 nM HGNs. This solution was allowed to react for 2 h by continuously stirring, so as to obtain an average yield of 72 adsorbed MGITC molecules per particle. In the following step, antibody conjugation was induced by the introduction of poly(ethylene glycol) 2-mercaptoethyl ether acetic acid (HS-PEG-COOH, MW ~3500) into the solution. HS-PEG-COOH was chemically bonded to the HGN surface by cleaving the SH terminal groups of HS-PEG-COOH. Consequently, a solution of 1 μL of 5.0 mM HS-PEG-COOH was added to 1 mL of 0.7 nM MGITC-adsorbed HGN, which was allowed to react for 1 h. Excess non-specifically bound HS-PEG-COOH molecules were removed from the solution using centrifugation. The precipitate was washed twice with PBS buffer and then re-suspended. Activation of the –COOH terminal groups was induced by mixing 1.0 μL of 5.0 mM EDC and 1.0 μL of 5.0 mM NHS and letting it react for 15 min. Protein molecules were stably immobilized on the carboxylate-terminated HGNs via the esterification of NHS with EDC. In the final step, 5.0 μL of 10 μM polyclonal anti-human IgG (excess amount) was added to the NHS-activated HGNs and allowed to react overnight at 4 °C. Lysine residues of the antibody displaced the NHS groups on the HGNs and

immobilized the antibodies. However, some molecules of the NHS groups on the surface of the HGNs had still not reacted, and so, deactivation was performed by the addition of 1.0 μL of 5 mM ethanolamine for 2 h. Non-specifically bound antibodies were removed by centrifugation. The nanoprobes thus obtained were then washed twice with a PBS buffer. Fig. S1 in the Electronic Supplementary Material (ESM) illustrates the sequential procedure for SERS nanotag production and their optical properties.

Preparation of CCP-conjugated magnetic beads

CCP-conjugated magnetic beads were prepared by streptavidin–biotin interaction. Five hundred microliters of 1.1 μg/mL biotinylated CCP was reacted with 500 μL of 0.5 mg/mL streptavidin-coupled magnetic beads (diameter= 1 μm). Biotinylated CCP was obtained from the working solution R1 in the Elecsys Anti-CCP kit, and the reaction was carried out for 2 h at room temperature. Five hundred microliters of 300 nM biotin was added to block any unreacted streptavidin. The unreacted reagents were removed by washing with PBS buffer solution.

Raman measurements

Raman measurements were performed using a Renishaw inVia Raman microscope system (Renishaw, UK). A Renishaw He–Ne laser, operating at a wavelength (λ) of 632.8 nm, was used as the excitation source with a laser power of 12.5 mW. A holographic notch filter located in the collection path was used to remove the Rayleigh line from the collected Raman scattering. The Raman scattering was collected using a charge-coupled device (CCD) camera. All spectra were calibrated to the 520 cm^{-1} silicon line. An additional CCD camera was fitted to an optical microscope to obtain optical images, and a ×20 objective lens was used to focus the laser on the glass tube. All of the reported Raman spectra were collected over 10-s exposure times in the range of 750~1840 cm^{-1}.

SERS-based immunoassay

The serum anti-CCP antibody marker concentration was estimated using the SERS-based immunoassays. Different solutions were prepared containing 20 μL of CCP-conjugated magnetic beads mixed with 40 μL of SERS nanotags. Varying concentrations of anti-CCP calibrator solution were added to the mixture. The resulting mixtures were incubated at room temperature for 45 min. After incubation, the immunocomplexes were isolated using a magnetic bar. A phosphate-buffered saline with Tween 20 (PBST) solution containing PBS and 0.01 % of Tween 20 was used as a wash buffer. The immunocomplexes were finally detached for the SERS analysis, which was carried out with 12 different concentrations of the anti-CCP autoantibody calibrator solutions that had been prepared for evaluation. The range of the concentrations for which the calibrator solutions were prepared were 0, 25, 50, 200, 800, and 3200 U/mL of the anti-CCP solutions (Immunoscan CCPlus, Euro Diagnostica). The lower concentrations of anti-CCP solutions, below 25 U/mL, were prepared by dilution of the calibrator solution.

ELISA immunoassay

An enzyme-linked immunosorbent assay was used as a confirmatory test to verify the accuracy of the SERS-based assay. To this effect, an ELISA test was performed according to the recommended protocol defined for the commercially available second-generation anti-CCP ELISA kit (Immunoscan CCPlus, Euro Diagnostica). A comparative analysis of the results from SERS-based immunoassay and ELISA was done.

Immunoassays of clinical serum samples

The assessment of diagnostic ability, clinical applicability, and analytical reproducibility of our proposed method was implemented on 74 clinical blood samples that were collected from patients with RA who had satisfied the American College of Rheumatology classification criteria [36], and from health volunteers at the Hanyang University Hospital. All human samples were handled in accordance with approved institutional review board (IRB) protocols at the hospital. An informed consent document was obtained from all volunteers included in this study. After collection, the samples were stored at −80 °C until use. The clinical samples were classified as anti-CCP-positive (n=31) and anti-CCP-negative (n=43) groups as per the anti-CCP quantification results obtained using an Immunoscan CCPlus (cutoff level, 25 U/mL). The manufacturer's recommendations were considered in order to gain the optimum results for the assay procedure. The anti-CCP level for each of the 74 clinical samples was also determined using the SERS immunoassay protocol. The SERS assay results were then compared with those measured by the ELISA method.

Statistical analysis of assay results

The analytical similarity and possible systematic differences between the two methods were estimated statistically. Passing–Bablok and Bland–Altman regression analyses were performed using MedCalc (Ostend, Belgium) for all clinical data [37, 38].

Results and discussion

Anti-CCP quantification using SERS-based immunoassay

The methods used to make the sandwich-type immunocomplexes for the SERS-based immunoassay are shown schematically in Fig. 1. When anti-CCP autoantibody markers are present in the serum, immunocomplexes form between the CCP-immobilized magnetic beads and the anti-human IgG-conjugated SERS nanotags. These immunocomplexes are formed through interactions among the CCP, anti-CCP, and anti-human IgG antibodies. However, a sandwich complex does not form in the absence of an anti-CCP target marker. The selectivity of the anti-CCP in the SERS-based immunoassay has been previously described [29]. When the SERS spectra were measured and analyzed for the same concentrations of anti-CCP, rheumatoid factor (RF), bovine serum albumin (BSA), and their mixtures, the SERS signals were observed only for the anti-CCP autoantibody and its mixtures. In contrast, no discernible Raman signals were observed for RF or BSA. Consequently, the amount of serum anti-CCP can be quantified by monitoring the Raman peak intensity of the SERS nanotags. Figure 2 illustrates the SERS-based immunoassay process used to quantify the anti-CCP autoantibody markers. Initially, biotinylated CCPs were immobilized by a biotin–streptavidin interaction on the surface of the streptavidin-coupled magnetic beads. Six different concentrations of biotinylated CCP (ranging between 110 and 2200 ng/mL) were reacted with 3200 ng/mL of anti-CCP (ESM Fig. S2) in order to identify the optimum CCP concentration. The SERS-based assay revealed the optimal CCP concentration to be 1100 ng/mL.

Next, different concentrations of anti-CCP autoantibodies were added to capture the CCPs. After the anti-CCP autoantibodies had been selectively captured on the surface of the magnetic beads, the secondary antibody-conjugated SERS nanotags were added. This step initiated the formation of the sandwich immunocomplexes. Finally, a magnetic bar on the wall of a microtube was used to attract and isolate the anti-CCP immunocomplexes. The residual solution was washed twice with a buffer using a micropipette. The magnetic bar was removed and the immunocomplexes dispersed for SERS measurements.

Assessment of SERS-based immunoassay

The evaluation of the analytical performance of the SERS-based assay was done by comparison with the commercially available and widely used Immunoscan CCPlus ELISA kit (Fig. 3). The Raman peak intensity was set at 1617 cm^{-1} in the quantitative evaluation by the SERS-based assay. On the overall, close agreement was observed for the SERS assay results (Fig. 3a) with those obtained using ELISA (Fig. 3d) for the anti-CCP solutions with concentrations above 25 U/mL.

However, for the assaying concentrations that were less than 25 U/mL, there was less correspondence between the SERS and ELISA data. At lower concentrations, a SERS-based assay outperformed the ELISA assay, and the SERS-based results were more consistent with the calculated concentrations than those that had been obtained by the ELISA analysis (Fig. 3b, e). This demonstrates that the SERS-based immunoassay technique allows for more sensitive quantification of the serum anti-CCP antibodies than does ELISA. The limit of detection (LOD) for the SERS-based immunoassay was estimated to be 0.18 U/mL, while that of ELISA was approximately 7.64 U/mL. The LODs were calculated at three standard deviations from the mean, using the standard calibration curve-fitting equation (Fig. 3c, f). Fig. S3 (ESM) displays the SERS spectra for various concentrations of the anti-CCP calibrator solution.

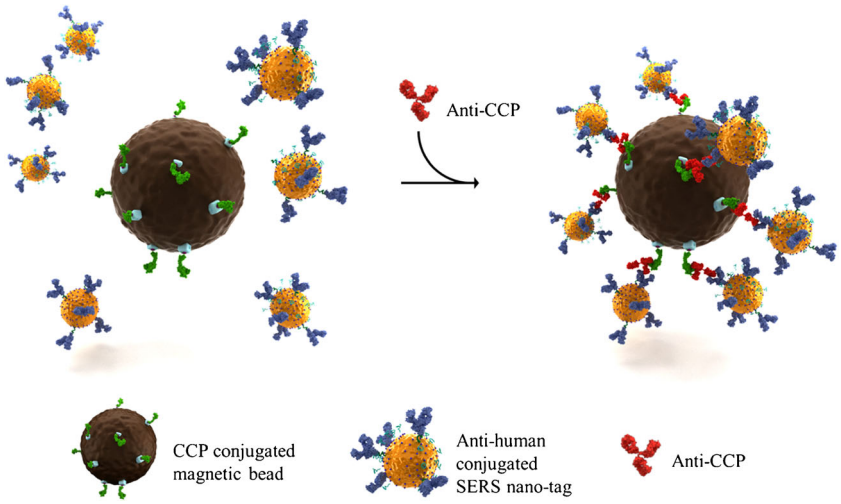

Fig. 1 Schematic illustration of the SERS-based immunoassay. When anti-CCPs are present in the serum, the CCP-conjugated magnetic beads and anti-human IgG-conjugated SERS nanotags form sandwich complexes by a CCP–anti-CCP–anti-human interaction

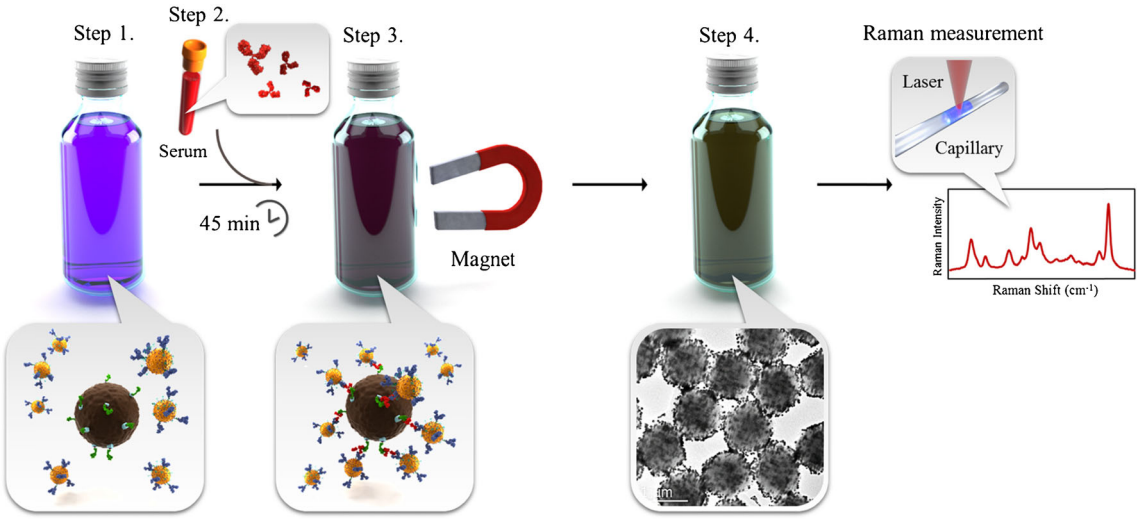

Fig. 2 SERS-based immunoassay procedure for the quantification of anti-CCP autoantibody markers. First, CCP-conjugated magnetic beads and SERS nanotags were mixed (*Step 1*). Serum containing anti-CCP autoantibodies was added to the solution (*Step 2*). After incubation for 45 min at room temperature, a magnetic bar was used to isolate the immunocomplexes. The remaining solution was washed with buffer (*Step 3*). Finally, the immunocomplexes were dispersed in PBS (*Step 4*), and Raman signals were measured

Fig. S4a (ESM) displays the quantitative assay results for ELISA and SERS-based assays using the normalized analysis in the 0~3200 U/mL range. The advantage of the SERS-based assay is in the low concentration regime, as the SERS-based results are more consistent with the calculated concentrations than those obtained by ELISA analysis. Fig. S4b (ESM) shows the distributions of standard deviation values determined by ELISA (blue) and SERS (orange) for all the clinical samples in the 0.1~3200 U/mL range. As shown in this figure, the SERS-based assay is characterized by a narrower distribution of standard deviations than for the ELISA data. Thus, it can be concluded that the SERS-based assay can be successfully applied to the sensitive and reproducible quantification of serum anti-CCP at all concentrations.

Evaluation of the SERS-based immunoassay for anti-CCP-positive clinical samples

To assess the clinical applicability of the proposed method, the SERS-based assays were performed on clinical blood samples

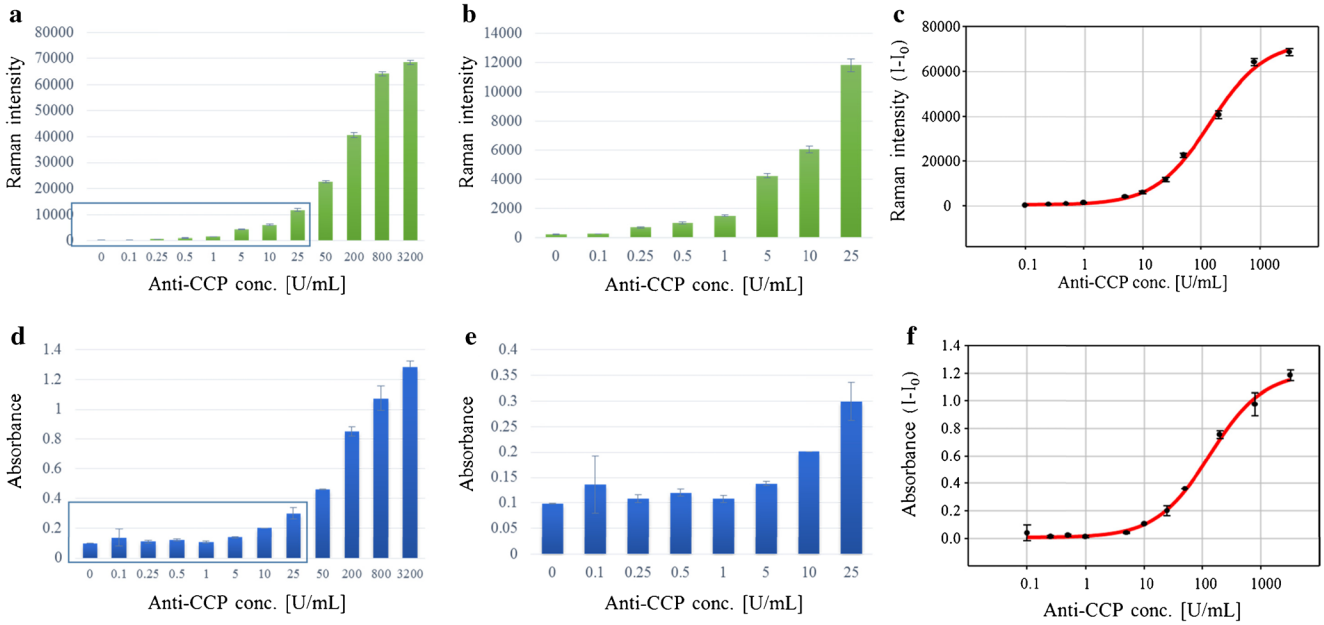

Fig. 3 The SERS intensity change at 1617 cm^{-1} as a function of anti-CCP concentration **a** in the 0~3200 U/mL range, **b** in the 0~25 U/mL range, and **c** the corresponding calibration curve determined by the SERS-based anti-CCP assay. Variation of absorbance as a function of anti-CCP concentration **d** in the 0~3200 U/mL range, **e** in the 0~25 U/mL range, and **f** the corresponding calibration curve determined by the commercially available ELISA kit. The *error bars* indicate standard deviations from three measurements

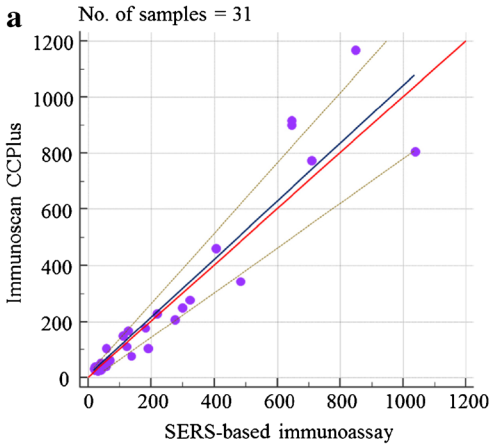

b

Regression line equation	$y = 7.11 + 1.03x$
95% CI for intercept	-14.20 ~ 15.82
95% CI for slope	0.80 ~ 1.25
Cusum test P value	P = 0.63
Cusum linearity test	No significant deviation from linearity

Fig. 4 A comparison of the quantitative assay results based on SERS and ELISA for anti-CCP-positive samples (n=31, >25 U/mL): **a** Passing–Bablok regression plot to determine the bias and comparability between SERS and ELISA. A solid blue line represents the regression line and two dotted lines give the 95% CI range. **b** Passing–Bablok regression results

and the results were compared to the ELISA data. First, the SERS-based immunoassay results from the anti-CCP-positive group (n=31, >25 U/mL) were compared with those obtained with the ELISA (using the Immunoscan CCPlus assay). In parallel, anti-CCP levels were determined using the SERS-based immunoassay on 31 clinical samples. Table S1 (ESM) displays the anti-CCP assay results for 31 human sera samples from the positive group. A Passing–Bablok regression analysis was also performed for the assay data shown in Table S1. Before performing the immunoassay on the clinical samples, anti-CCP calibration curves for both ELISA and SERS-based assays were generated using anti-CCP calibrators of known concentration (Fig. 3c, f). In the SERS-based assay, the Raman intensity at 1617 cm^{-1} was implemented and the calculation of the anti-CCP concentration was done using the calibration fitting equation.

A Passing–Bablok regression analysis was used to estimate the similarity and possible systematic differences between the two different analytical methods. Panels a and b of Fig. 4 establish good conformity between the two analytical methods if the 95 % confidence intervals (CIs) for the intercept and the slope include 0 and 1, respectively. Figure 4a shows the scatter (purple points) and regression (blue line) plots. Ninety-five percent CIs for the intercept and the slope were determined to range between −14.20~15.82 and 0.80~1.25 U/mL, respectively. From the relatively small interval for the intercept and the large P value (P=0.63), we can conclude that the correlation for the positive patient group is good. The 95 % CI values satisfy both conditions, indicating that all values are within the clinically acceptable range (15~1200 U/mL). These results imply that the SERS-based immunoassay is clinically acceptable for the anti-CCP-positive group (n=31), since all of the difference values in the Passing–Bablok regression analysis are within acceptable ranges.

Evaluation of SERS-based immunoassay for anti-CCP-negative clinical samples

As shown in Fig. 3, the SERS-based immunoassay is more accurate than ELISA when applied to standard anti-CCP solutions of low concentration (0~25 U/mL). In order to determine whether or not the SERS-based assay has clinical value in the early diagnosis of RA, we also applied it to the anti-CCP-negative group (n=43). As before, we compared these results to those obtained using ELISA. Unfortunately, there was no gold standard to confirm the anti-CCP levels in the negative patient group. Instead, a statistical analysis was used to compare the two analytical methods. Table 1 displays the anti-CCP assay results for 43 human sera samples from the negative group. A Passing–Bablok regression analysis was also performed for the assay data in Table 1. This analysis did not reveal a good correlation between the two analytical methods (Fig. 5a). The 95 % CIs for the intercept and the slope were determined to range between −6.35~2.52 and 0.04~1.07 U/mL, respectively. From the large interval for the intercept and the small P value (P= 0.01), we can conclude that the correlation for the negative patient group is not strong. The Bland–Altman analysis in Fig. 5b also shows a mean difference of −4.3 U/mL and 95 % limit of agreement in the –24.9~16.4 U/mL range. Accordingly, we can conclude that there is a strong correlation between the SERS-based assay and ELISA for the anti-CCP-positive group (n=31); however, no such correlation exists for the negative group (n=43). Panels d and e of Fig. 5 display the standard deviations of the anti-CCP levels obtained in 43 negative clinical samples using the ELISA and SERS-based assays. Here, the amount of the anti-CCP was determined using the calibration curves in Fig. 3c, f. The SERS-based assay is characterized by a narrower distribution of standard deviations than for the ELISA data since the SERS data has a more precise calibration

Table 1 Comparison of the quantitative results determined by ELISA and SERS-based immunoassays for anti-CCP-negative clinical samples (n=43, <25 U/mL)

Sample no.	ELISA		SERS-based assay	
	$y = y_0 + \frac{a}{1+\left(\frac{x}{x0}\right)^b}$		$y = y_0 + \frac{a}{1+\left(\frac{x}{x0}\right)^b}$	
	y_0=0.3110		y_0=546.04	
	x_0=152.2563		x_0=139.99	
	a =0.7042		a =73,001.72	
	b =−1.1163		b =−0.9328	
	Concentration (U/mL)	CV (%)	Concentration (U/mL)	CV (%)
1	18.3	13.71	26.29	7.43
2	8.1	22.62	2.27	6.43
3	18.6	18.01	10.54	5.14
4	9.5	12.36	8.02	9.98
5	6.6	21.4	1.74	8.26
6	10.13	8.58	0.12	4.15
7	9.14	10.25	1.40	7.25
8	0.00	17.2	0.66	8.7
9	0.00	0.1	10.16	12.71
10	10.30	10.73	4.33	6.16
11	4.13	18.32	0.66	7.16
12	24.91	3.99	6.97	4.42
13	7.47	5.32	0.29	5.43
14	10.79	18.58	2.25	5.13
15	0.00	16.35	2.64	4.08
16	7.13	7.55	3.33	9.13
17	6.27	31.05	0.26	6.72
18	15.13	22.99	5.90	9.44
19	0.00	8.79	0.77	6.03
20	15.60	31.13	7.44	9.32
21	2.62	25.66	2.43	11.87
22	0.00	17.6	10.43	5.28
23	0.00	8.63	13.95	10.22
24	0.93	14.15	22.44	8.61
25	0.00	18.76	11.79	8.04
26	2.81	9.1	13.49	5.03
27	1.16	19.11	19.17	6.64
28	0.00	6.05	6.38	11.58
29	4.86	11.52	10.48	11.49
30	6.27	19.64	24.93	11.17
31	0.00	14.5	12.92	5.98
32	7.13	11.17	10.98	6.2
33	2.22	11.66	19.17	6.33
34	1.38	22.55	26.59	9.28
35	0.00	12.09	12.66	6.85
36	0.00	9.05	14.95	6.17
37	0.00	6.07	17.80	8.22
38	0.00	18.63	6.75	7.69

Table 1 (continued)

Sample no.	ELISA		SERS-based assay	
	$y = y_0 + \frac{a}{1+\left(\frac{x}{x0}\right)^b}$		$y = y_0 + \frac{a}{1+\left(\frac{x}{x0}\right)^b}$	
	y_0=0.3110		y_0=546.04	
	x_0=152.2563		x_0=139.99	
	a =0.7042		a =73,001.72	
	b =−1.1163		b =−0.9328	
	Concentration (U/mL)	CV (%)	Concentration (U/mL)	CV (%)
39	4.13	16.33	24.82	9.83
40	2.01	14.63	9.49	6.21
41	14.17	13.85	9.35	7.31
42	0.00	15.48	9.35	12.7
43	0.00	11.54	8.28	9.39
Mean	5.39	14.58	9.64	7.79

curve in the low concentration range (0~25 U/mL) (Fig. 3). Based on our results, we therefore conclude that the SERS-based assay can be successfully applied for the sensitive and reproducible quantification of serum anti-CCP, especially at low concentrations (<25 U/mL). In the case of ELISA, it is reported as "negative" when the anti-CCP level in serum is

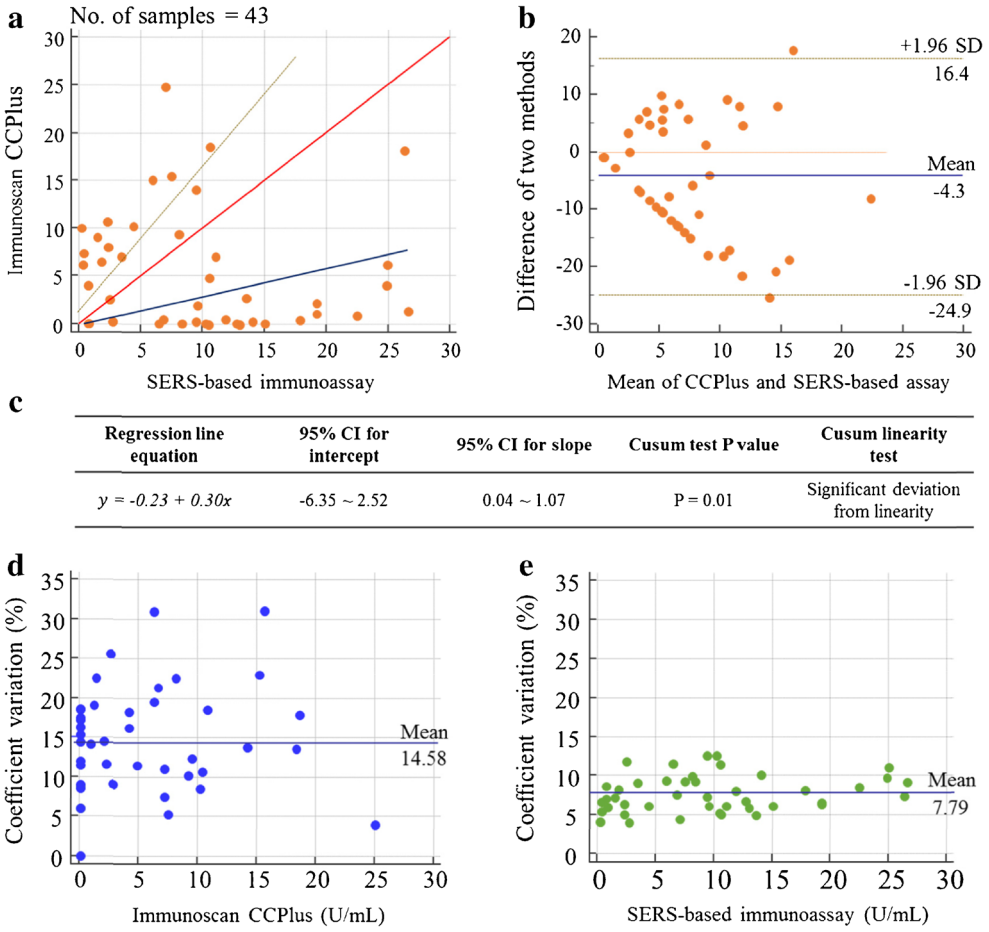

Fig. 5 A comparison of the quantitative assay results between SERS and ELISA for anti-CCP-negative samples (n=43, <25 U/mL): **a** Passing–Bablok regression plot; fitting equation, y=−0.23+0.30x; 95 % confidence intervals for intercept, −6.35~2.52; and 95 % confidence intervals for slope, 0.04~1.07. **b** Bland–Altman plot for the assay results determined by SERS and ELISA. A *solid horizontal blue line* represents the mean difference of −4.3 U/mL, and *two dotted horizontal lines* give the 95 % limits of agreement in the −24.9~16.4 U/mL range. **c** Passing–Bablok regression results. Distributions of the standard deviation values determined by **d** ELISA and **e** SERS

lower than 25 U/mL. As mentioned in the "Introduction," however, a highly accurate assay technique in the low anti-CCP concentration range (<25 U/mL) is important for the early diagnosis of RA. Our results suggest that the SERS-based assay has a strong potential to be a valuable tool for the early diagnosis of RA, because this assay shows more consistent results than did ELISA for the anti-CCP-negative group.

Conclusions

This study reveals a novel SERS-based immunoassay technique for the highly sensitive and reproducible quantification of anti-CCP. CCP-conjugated magnetic beads were used as substrates, while anti-human IgG-conjugated HGNs were used as SERS nanotags. The amount of the anti-CCP markers in the serum was successfully quantified by monitoring the characteristic Raman peak intensity of the SERS nanotags. The anti-CCP levels that were determined by our proposed SERS assay method complied strongly with those of the ELISA kit in the high anti-CCP concentration range (>25 U/mL). In addition, our SERS-based assay results are more consistent in the low concentration range (<25 U/mL) than those achieved by the commercial ELISA kit, making the SERS-based assay a more reliable and robust alternative to traditional diagnostic tests.

The clinical performance of the anti-CCP assays was tested on 74 clinical blood samples. The SERS-based assay results were compared with those obtained from conventional ELISA analysis. There was a good correlation between the ELISA and SERS-based data in the anti-CCP-positive group (n= 31, >25 U/mL). However, the SERS-based assay demonstrated superior reproducibility in the negative group (n= 43, <25 U/mL).

To replace the immunoassay systems currently in use with the SERS-based assay platform in the near future, some of the problems, including the fabrication and mass production of highly reproducible SERS nanotags, and the development of an automatic Raman sampling system for clinical analysis, should be solved. In this study, we extended the feasibility of the SERS-based assay technique to carry out an anti-CCP marker assay in clinical samples for the early diagnosis of RA. On the overall, these results suggest that the SERS-based assay has the potential to become a valuable tool in the early diagnosis of RA.

Acknowledgments This work was supported by the National Research Foundation of Korea (Grant Numbers 2008-0061856 and 2009-00426) and by the Nano Materials Technology Development Program through the National Research Foundation of Korea. The study was funded by the Ministry of Education, Science and Technology (Grant Number 2012M3A7B4035288). H.C. acknowledges the financial support (Grant Number 2013R1A1A2063269) of the National Research Foundation of Korea.

Conflict of interest The authors declare that they have no competing interests.

References

1. Porter MD, Lipert RJ, Siperko LM, Wang G, Narayana R (2008) Chem Soc Rev 37:1001–1011
2. Han XX, Cai LJ, Guo J, Wang CX, Ruan WD, Han WY, Xu WQ, Zhao B, Ozaki Y (2008) Anal Chem 80:3020–3024
3. Lee M, Lee S, Lee JH, Lim HW, Seong GH, Lee EK, Chang SI, Oh CH, Choo J (2011) Biosens Bioelectron 26:2135–2141
4. Gong JL, Liang Y, Huang Y, Chen JW, Jiang JH, Shen GL, Yu RQ (2007) Biosens Bioelectron 22:1501–1507
5. Driskell JD, Kwarta KM, Lipert RJ, Porter MD, Neill JD, Ridpath JF (2005) Anal Chem 77:6147–6154
6. Wang G, Park HY, Lipert RJ, Porter MD (2009) Anal Chem 81: 9643–9650
7. Yang J, Palla M, Bosco FG, Rindzevicius T, Alstrøm TS, Schmidt MS, Boisen A, Ju J, Lin Q (2013) ACS Nano 7:5350–5359
8. Li M, Cushing SK, Zhang J, Suri S, Evans R, Petros WP, Gibson LF, Ma D, Liu Y, Wu N (2013) ACS Nano 7:4967–4976
9. Li T, Guo L, Wang Z (2008) Biosens Bioelectron 23:1125–1130
10. Ni J, Lipert RJ, Dawson GB, Porter MD (1999) Anal Chem 71: 4903–4908
11. Grubisha DS, Lipert RJ, Park HY, Driskell J, Porter MD (2003) Anal Chem 75:5936–5943
12. Lin CC, Yang YM, Chen YF, Yang TS, Chang HC (2008) Biosens Bioelectron 24:178–183
13. Xu SP, Ji XH, Xu WQ, Li XL, Wang LY, Bai YB, Zhao B, Ozaki Y (2004) Analyst 129:63–68
14. Wang G, Lipert RJ, Jain M, Kaur S, Chakraboty S, Torres MP, Batra SK, Brand RE, Porter MD (2011) Anal Chem 83:2554–2559
15. Yoon J, Choi N, Ko J, Kim K, Lee S, Choo J (2013) Biosens Bioelectron 47:62–67
16. Chung E, Jeon J, Yu J, Lee C, Choo J (2015) Biosens Bioelectron 64:560–565
17. Ko J, Lee C, Choo J (2015) J Hazard Mater 285:11–17
18. Gao R, Ko J, Cha K, Jeon JH, Rhie G, Choi J, deMello AJ, Choo J (2015) Biosens Bioelectron 72:230–236
19. Ye J, Chen Y, Liu Z (2014) Angew Chem Int Ed 53:10386–10389
20. Wang Y, Rauf S, Grewal YS, Spadafora LJ, Shiddiky MJA, Cangelosi GA, Schlucker S, Taru M (2014) Anal Chem 86:9930–9938
21. Lee S, Chon H, Lee M, Choo J, Shin SY, Lee YH, Rhyu IH, Son SW, Oh CH (2009) Biosens Bioelectron 24:2260–2263
22. Huang J, Kim KH, Choi N, Chon H, Lee S, Choo J (2011) Langmuir 27:10228–10233
23. Chon H, Lee S, Son SW, Oh CH, Choo J (2009) Anal Chem 81: 3029–3034
24. Chon H, Lee S, Yoon SY, Chang SI, Lim DW, Choo J (2011) Chem Commun 47:12515–12517
25. Chon H, Lee S, Yoon SY, Lee EK, Chang SI, Choo J (2014) Chem Commun 50:1058–1060
26. Angenendt P (2005) Drug Discov Today 10:503–511
27. Lee M, Kim KH, Park JG, Lee JH, Lim HW, Park MY, Chang SI, Lee EK, Lim DW, Choo J (2012) Biochip J 6:10–16
28. Kanda V, Kariuki JK, Harrison DJ, McDermott MT (2004) Anal Chem 76:7257–7262
29. Chon H, Lee S, Wang R, Bang SY, Lee HS, Bae SC, Lee H, Kim B, Choo J (2014) RSC Adv 4:32924–32927
30. Nijenhuis S, Zendman AJW, Vossenaar ER, Pruijn GJM, van Venrooij WJ (2004) Clin Chim Acta 350:17–34

31. Bossuyt X, Coenen D, Fieuws S, Verschueren P, Westhovens R, Blanckaert N (2009) Ann Rheum Dis 68:287–289
32. Jaskowski TD, Hill HR, Russo KL, Lakos G, Szekanecz Z, Teodorescu M (2010) J Rheumatol 37:1582–1588
33. Chon H, Lee S, Wang R, Bang SY, Lee HS, Bae SC, Hong SH, Yoon YH, Lim D, Choo J (2015) Highly sensitive immunoassay of anti-cyclic citrullinated peptide marker using surface-enhanced Raman scattering detection. Proc SPIE 9523:95230J. doi:10.1117/12.2189760.
34. Schwartzberg AM, Oshiro TY, Zhang JZ, Huser T, Talley CE (2006) Anal Chem 78:4732–4736
35. Wang H, Goodrich GP, Tam F, Oubre C, Nordlander P, Halas NJ (2005) J Phys Chem B 109:11083–11087
36. Arnett FC, Edworthy SM, Bloch DA, McShane DJ, Fries JF, Cooper NS, Healey LA, Kaplan SR, Liang MH, Luthra HS (1988) Arthritis Rheum 31:315–324
37. Bland JM, Altman DG (1986) Lancet 1:307–310
38. Passing H, Bablok W (1983) J Clin Chem Clin Biochem 21:709–720